THE PREDICTION OF ELECTROCHEMICAL REACTIVITIES FROM CONTEMPORARY THEORY:
SOME COMPARISONS WITH EXPERIMENT

J.T. HUPP[1], H.Y. LIU[2], J.K. FARMER[2], T. GENNETT[1] and M.J. WEAVER[1*]

[1]Dept. of Chemistry, Purdue University, West Lafayette, Indiana 47907 (USA)

[2]Graduate Research Assistant, Michigan State University (USA)

ABSTRACT

The application of current theoretical treatments of electron transfer to
outer-sphere electrochemical reactions are considered with regard to the
numerical prediction of rate parameters from thermodynamic and structural
data. Formalisms based on a "semiclassical" treatment for the Franck-Condon
barrier together with an "encounter preequilibrium" model for the pre-
exponential factor are summarized and related to the more widely considered
treatments for homogeneous redox reactions. Comparisons are made between
the theoretical predictions and experimental rate parameters for representa-
tive inorganic outer-sphere reactions at electrode surfaces, and with
relative reactions in homogeneous solution. The effects of altering the
electrode material and the outer-shell solvent are also considered.
Although the measured rate parameters for several reactions at mercury
electrodes are in reasonable agreement with the theoretical predictions,
significant and even large discrepancies are seen for a number of cases.
Likely reasons for these findings are discussed, including nonadiabaticity
and specific solvation effects.

INTRODUCTION

Theoretical treatments of electron-transfer processes in condensed media
have undergone considerable development in recent years [1]. Although these
activities have been concerned with a diverse range of conceptual problems
and practical systems, much attention has been focussed on treating outer-
sphere processes involving pairs of transition-metal reactants in
homogeneous solutions [1d-f]. There are several reasons for this emphasis.
Firstly, the ingenuity of inorganic chemists both in synthesizing a wide
variety of structurally well-defined one-electron redox couples and in
devising methods for obtaining detailed kinetic and mechanistic information
has yielded a rich body of experimental rate data. Secondly, the structural
simplicity and varied electronic properties of these reactants have

---

*Author to whom correspondence should be addressed.

attracted the attention of theoretical chemical kineticists [1a-c,e]. Outer-sphere electron transfer in general constitutes an especially tractable situation since the potential-energy surfaces of the two reactants can be treated independently in the absence of chemical interactions between redox centers (the "weak overlap" case). Thirdly, the widespread importance of transition-metal redox processes in chemistry and biology, along with the remarkably wide range (ca 10^{20}) of rate constants encountered for such systems, has spurred on efforts to obtain a quantitative understanding of the observed reactivities [1f].

Although outer-sphere reactions involving transition-metal complexes at metal surfaces and in homogeneous solution are closely related processes, such systems have not been blessed with the same detailed attention that has benefited the homogeneous redox area [2]. This is unfortunate since studies of such simple reactions at metal surfaces can yield much insight into the nature of charge-transfer processes. In addition, comparative studies of these reactants at metal surfaces and in bulk solution offer special opportunities for exploring the similarities and differences between homogeneous and heterogeneous redox reagents (i.e., electrodes).

Studies of outer-sphere electron transfer received an early impetus from the work of Marcus [3], who demonstrated that several simple relationships might be expected to hold between the rates of related cross- and self-exchange reactions in homogeneous solution, and with the corresponding electrochemical reactions at varying overpotentials. While these relationships are important and useful in a practical sense, much experimental work has been directed solely towards checking their applicability; (the "relative predictions" of electron-transfer theory [4]). Moreover, the demonstrated applicability of these relationships, at least approximately, to a fairly wide variety of reactions has generated the impression that the quantitative understanding of electron-transfer reactivity is largely a "solved problem". This misconception arises in part from the insensitivity of these "relative predictions" to the theoretical models employed, due to an extensive cancellation of terms that is inherent to such relative-rate comparisons.

A much more critical test of electron-transfer theories involves their ability to predict rate parameters for individual reactions. Such "absolute" rate comparisons [4] between theory and experiment have been sparse. This has been due primarily to the paucity of the bond length and vibrational data that are necessary in order to calculate the inner-shell component of the free-energy barrier (i.e., that associated with the reorganization of the bonds within the reactant species). However, this situation has now

varied by altering the applied electrode potential, E, relative to the standard potential, $E°$.

According to the encounter preequilibrium model, the observed rate constant, k_{ob}, for either an electrochemical or homogeneous reaction can be expressed as [7-10]:

$$k_{ob} = K_p k_{et} \qquad (2a)$$

where K_p is an equilibrium constant for the formation of the "precursor" (encounter preequilibrium) state from the separated reactants, and k_{et} (s^{-1}) is the unimolecular rate constant for the electron-transfer step between the reactants within this encounter state. For outer-sphere reactions, it is particularly convenient to define a "work-corrected" rate constant k_{corr}, which would equal k_{ob} in the absence of electrostatic work terms. Approximate values of k_{corr} can be obtained from k_{ob} for electrochemical or homogeneous reactions by using the Gouy-Chapman or Debye-Huckel models, respectively. Equation (2a) can then be written as:

$$k_{corr} = K_o k_{et}^{corr} \qquad (2b)$$

where K_o and k_{et}^{corr} are the work-corrected values of K_p and k_{et}, respectively. The exact form of the expressions for K_p and K_o depends on the ability of the transferring electron to tunnel between the donor and acceptor sites, and also upon the presence of any electrostatic interactions between the reactants [10]. However, an approximate relationship can be deduced by assuming that there is a reaction zone around one reactant (or the electrode) within which the reactant needs to be situated in order to contribute to the reaction rate. For electrochemical reactions, the value of K_o, K_o^e, is simply [10]:

$$K_o^e = \delta r_e \qquad (3)$$

where δr_e is the effective reaction zone thickness (cm). For homogeneous reactions, an analogous expression has been advocated [5,7b]:

$$K_o^h = 4\pi N r_h^2 \, \delta r_h \qquad (4)$$

where N is Avogadro's constant, r_h is the contact distance between the (spherical) reactions, and δr_h is the reaction zone thickness around each reactant. The more complex nature of equation (4) versus equation (2) reflects the spherical rather than the planar shape of the reaction zone for homogeneous processes. It is important to recognize that the encounter preequilibrium model is based on a distinctly different physical treatment to the collisional model which has been commonly used in the past. Indeed,
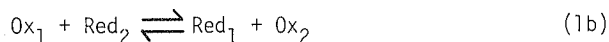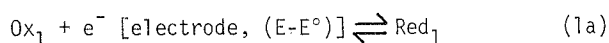
changed. The degree of alteration in metal-ligand bond distances accompanying electron transfer have recently become available for a number of transition-metal redox couples from solution EXAFS as well as X-ray crystallographic measurements [5]. These structural data have been utilized to calculate rate constants for a number of homogeneous self-exchange reactions. Broad agreement between the theoretical and experimental rate constants was claimed [5,6].

These recent studies also employ a contemporary electron-transfer model which considers the free-energy barrier to be surmounted by means of a unimolecular activation process within a previously formed "encounter complex" [7,10], in place of the more conventional collisional model that has previously been employed [3,7a]. We have recently shown that essentially the same "encounter preequilibrium" model can be employed for outer-sphere electrochemical reactions [10]. This approach facilitates the examination of electrochemical and homogeneous processes on a common basis, including those following inner- rather than outer-sphere pathways [10].

In view of these developments, it seems timely to explore the ability of contemporary electron-transfer models to predict outer-sphere electrochemical reactivities. The purpose of this conference paper is to review the physical features of these models and the resulting numerical relationships for one-electron electrochemical reactions, along with some comparisons between the calculated rate parameters and experimental data for simple inorganic systems. Particularly since further experimental and calculational details of this material are [10-12] or shortly will be available elsewhere, the following is intended to summarize and illustrate some key current issues, rather than to provide a comprehensive report.

THEORETICAL TREATMENT

We shall consider the related one-electron electrochemical and homogeneous reactions as depicted in equations (1a) and (1b) respectively:

$$Ox_1 + e^- \text{ [electrode, } (E-E^\circ)] \rightleftharpoons Red_1 \qquad (1a)$$

$$Ox_1 + Red_2 \rightleftharpoons Red_1 + Ox_2 \qquad (1b)$$

Although most theoretical work has been formulated for bimolecular homogeneous reactions, the key ideas can be transposed to electrochemical processes by formally treating the electrode surface as one of the reactants. The major differences are that the electrode, unlike solution reactants, need not be activated and the reaction thermodynamics can be continuously

distinctly different values of the overall preexponential factors are obtained from these two approaches [10].

The unimolecular rate constant k_{et}^{corr} can generally be expressed as [1f,10]:

$$k_{et}^{corr} = \nu_n \Gamma_n \kappa_{el} \exp(-\Delta G^*/RT) \qquad (5)$$

where ν_n is a nuclear frequency factor (s^{-1}), Γ_n is a nuclear tunneling factor, κ_{el} is an electronic transmission coefficient, and ΔG^* is the free energy of activation for the elementary electron-transfer step. The two "quantum-mechanical" tunneling factors Γ_n and κ_{el} represent corrections to the classical electron-transfer model, yielding the so-called "semi-classical" treatment [6] embodied in equation 5. The former quantity represents the correction to the rate constant from molecules that react without fully surmounting the electron-transfer barrier. The latter term denotes the probability that electron transfer will occur once the nuclear transition state has been reached. For so-called "adiabatic pathways", $\kappa_{el} \sim 1$; however, poor overlap between the donor and acceptor orbitals can force the overall reaction to occur by a "nonadiabatic pathway", where $\kappa_{el} \ll 1$, even when the redox centers are in contact [1e,13,14].

The theoretical estimation of κ_{el} for nonadiabatic pathways is difficult, and has not yet been attempted satisfactorily for electrochemical processes. However, relatively reliable values of Γ_n and ν_n can be calculated. Although the relationships for the former are complicated, approximate analytical expressions have been devised [1f]. At least for reactions having small or moderate inner-shell barriers (≤ 40 kJ mol^{-1}), Γ_n is close to unity at ambient temperatures ($\Gamma_n \sim 1-3$). The nuclear tunneling component associated with solvent reorganization will almost always be negligible due to the typically small barriers (~ 20 kJ mol^{-1}) together with the low characteristic frequencies of solvent reorientation. The nuclear frequency factor can be estimated from [10]:

$$\nu_n^2 = (\nu_{os}^2 \Delta G_{os}^* + \nu_{is}^2 \Delta G_{is}^*)/(\Delta G_{os}^* + \Delta G_{is}^*) \qquad (6)$$

where ν_{os} and ΔG_{os}^* are the characteristic frequency and free energy of activation associated with outer-shell (solvent) reorganization, and ν_{is} and ΔG_{is}^* are the corresponding quantities associated with inner-shell (reactant bond) vibrations. Although ν_{os} and ν_{is} are markedly different (typically ca $10^{11} - 10^{12}$ and 10^{13} s^{-1}, respectively [5,6]), equation (6) yields ν_n values which commonly are close to 1×10^{13} s^{-1} even when $\Delta G_{os}^* > \Delta G_{is}^*$. The expressions for Γ_n and ν_n appropriate for electrochemical processes are identical to those for homogeneous reactions, although those for the latter necessarily employ parameters (such as vibrational

frequencies and free-energy barriers) which include contributions from both reactants.

The classical "Franck-Condon" barrier $\Delta G^\star$ (equation (4)) is usually considered to consist of separate additive contributions from the (inner-shell) distortions of the reacting species, $\Delta G^\star_{is}$, and the (outer-shell) reorientation of the surrounding solvent, $\Delta G^\star_{os}$. Marcus demonstrated that the calculation of both of these quantities is greatly facilitated by evaluating a component of the barrier associated with an overall free energy driving force, ΔG°, equal to zero (the "intrinsic barrier"). The value of $\Delta G^\star$ at the desired driving force ΔG° can then be found from the overall intrinsic barrier, $\Delta G^\star_{int}$, suitably modified by inclusion of an appropriate functional relationship between $\Delta G^\star$ and ΔG° [3]. The intrinsic barrier for electrochemical reactions corresponds to $\Delta G^\star$ at the standard potential E°, since then $|\Delta G^\circ| = |F(E-E^\circ)| = 0$.

The outer-shell intrinsic barrier, $\Delta G^\star_{os,int}$, is usually obtained by using a nonequilibrium dielectric continuum treatment. For electrochemical reactions it is expressed as [3]:

$$\Delta G^\star_{os,int} = \frac{Ne^2}{8} \left(\frac{1}{a} - \frac{1}{R_e}\right)\left(\frac{1}{\varepsilon_{op}} - \frac{1}{\varepsilon_s}\right) \qquad (7)$$

where a is the reactant radius; R_e is twice the reactant-electrode distance; and ε_{op} and ε_s are the optical and static dielectric constants of the surrounding solvent.

The simplest approach to calculating the inner-shell intrinsic barrier, $\Delta G^\star_{is,int}$, for electrochemical reactions is to employ the relation (cf. [5])

$$\Delta G^\star_{is,int} = 0.5 \sum f'_i (\Delta a/2)^2 \qquad (8)$$

where Δa is the difference in the bond distance between the oxidized and reduced forms of the redox couple, and f'_i is the "reduced" force constant of the i th bond; this is related to the individual force constants of these bonds in the oxidized and reduced states by $f'_i = 2f_{ox}f_{red}/(f_{ox} + f_{red})$ [5]. These individual force constants, f_i, can be calculated from the appropriate vibrational frequencies, ν_i, obtained by means of infrared or, preferably, Raman spectroscopy using

$$f_i = 4\pi^2\nu_i^2 c^2\mu \qquad (9)$$

where c is the velocity of light and μ is the effective (reduced) mass of the vibrating group. Equation (8) yields values of $\Delta G^\star_{is,int}$ that are exactly one half of those calculated for homogeneous reactions [5], as
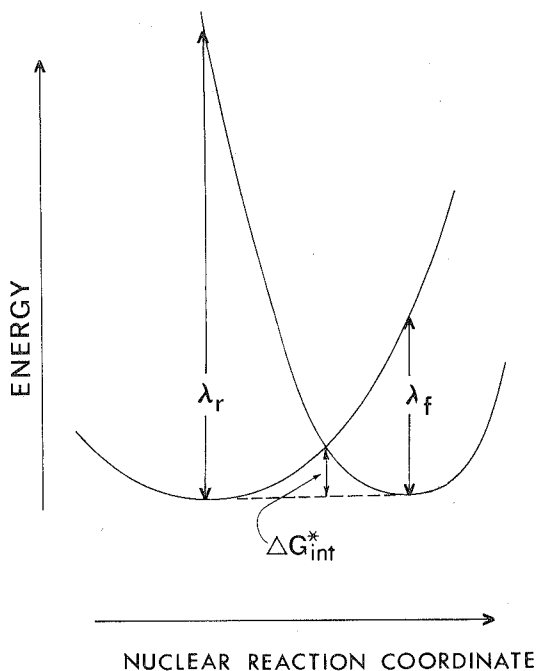
Fig. 1. Schematic representation of the forward and reverse organization energies, λ_f and λ_r, respectively, and relationship to the intrinsic barrier, ΔG^*_{int}.

expected since only one reactant is required to be activated for electro-chemical reactions.

Although equation (8) provides a good approximation to the inner-shell barrier for reactions at small driving forces (i.e., small overpotentials) and/or for small or moderate differences between f_{ox} and f_{red}, a preferable approach is to calculate $\Delta G^*_{is,int}$ from the *individual* free-energy curves for the oxidized and reduced states. For this purpose, it is useful to define so-called intrinsic reorganization energies, λ_f and λ_r, for the forward and reverse reactions, respectively [3]. These quantities are shown schematically in Fig. 1; λ_f equals the free energy required to reorganize the nuclear (reactant bond and solvent) coordinates of the reactant(s) so that they match those of the product(s), and λ_r is the same quantity for the reverse reaction. Both λ_f and λ_r refer to the condition $\Delta G° = 0$, i.e., for $E = E°$ (Fig. 1).

For electrochemical reactions [equation (1a)] λ_f and λ_r are given by Marcus' additivity rules as [3]:

$$\lambda_f = \lambda_{is}^{Ox} + \lambda_{os} \qquad (10a)$$

and

$$\lambda_r = \lambda_{is}^{Red} + \lambda_{os} \qquad (10b)$$

where λ_{is}^{Ox} and λ_{is}^{Red} are the inner-shell reorganization energies for the forward and reverse reactions (i.e., for the oxidized and reduced states) and λ_{os} is the outer-shell reorganization energy, equal to $4\Delta G_{os,int}^{*}$ [3]. For homogeneous reactions [equation (1b)], λ_f and λ_r will contain contributions from both the reactants, so that

$$\lambda_f = \lambda_{is}^{Ox_1} + \lambda_{is}^{Red_2} + \lambda_{os} \qquad (11a)$$

$$\lambda_r = \lambda_{is}^{Red_1} + \lambda_{is}^{Ox_2} + \lambda_{os} \qquad (11b)$$

Although λ_{os} is assumed to be the same for the forward and reverse reactions, λ_{is}^{Ox} and λ_{is}^{Red} will generally differ since $f_{ox} \neq f_{Red}$. The general relation between λ_{is} and the bond force constants is [cf. equation (8)]:

$$\lambda_{is} = 0.5 \; \Sigma \; f_i \; (\Delta a)^2 \qquad (12)$$

where f_i is now the individual force constant for the i th vibrating bond in the appropriate oxidation state.

If the outer- as well as inner-shell reorganization energies are taken to be quadratic functions of the nuclear coordinates, the required free energy of activation ΔG^* can be obtained from the intersection point of the reactant and product parabolas for the appropriate free energy driving force ΔG° [$=F(E-E^\circ)$] [3]. This is conveniently expressed as:

$$\Delta G^* = \lambda_f X^2 \qquad (13a)$$

where

$$\lambda_f X^2 = \lambda_r (1-X)^2 + \Delta G^\circ \qquad (13b)$$

These relations apply to both electrochemical and homogeneous processes. If $\lambda_f \approx \lambda_b = \lambda$ when $\Delta G^\circ = 0$ so that ΔG^* equals the intrinsic barrier ΔG_{int}^*, we find that

$$\Delta G_{int}^* = \lambda/4 \qquad (14)$$

which along with equation (12) yields the simplified equation (8). However, the more complete treatment is to be preferred. This is especially true for reactions at moderate or large values of ΔG°, where equation (13)

predicts noticeably different dependencies of ΔG^* (and hence log k_{ob}) upon the sign as well as the magnitude of the driving force if $\lambda_f \neq \lambda_r$ (*vide infra*).

The above relations enable calculated values of k_{corr}, k_{calc}, to be obtained for outer-sphere electrochemical reactions as a function of the thermodynamic driving force (i.e., the cathodic or anodic overpotential), providing that the required values of ν_i and Δa for each bond undergoing distortion during electron transfer are known, or can be estimated. In addition to considering the rate constants themselves, it is instructive to compare the activation parameters predicted from theory with the corresponding experimental values. Although a measure of confusion has surrounded the interpretation of electrochemical activation parameters, in actuality they contain no more ambiguity than the commonly encountered quantities for homogeneous redox processes [15,16]. Particularly relevant to the present purpose are the so-called "real" activation parameters obtained from the temperature dependence of the standard rate constant k_{corr}^S, i.e., the electrochemical rate constant determined at E° [or at a constant overpotential $\eta = (E-E^\circ)$] at *each* temperature. (These quantities should be distinguished from the so-called "ideal" activation parameters obtained from the temperature dependence of the rate constant at a fixed metal-solution potential difference. The latter contain an additional entropic driving force term, and are most usefully evaluated for chemically irreversible electrochemical reactions for which E°, and hence "real" activation parameters, cannot be determined [15].)

From equations (2b), (3), and (5) we can write for electrochemical reactions:

$$k_{corr}^S = \delta r_e \, \nu_n \Gamma_n \kappa_{el} \, \exp\left(-\Delta G_{int}^*/RT\right) \tag{15a}$$

$$= \delta r_e \, \nu_n \Gamma_n \kappa_{el} \, \exp\left(\Delta S_{int}^*/R\right) \exp\left(-\Delta H_{int}^*/RT\right) \tag{15b}$$

where ΔS_{int}^* and ΔH_{int}^* are the entropic and enthalpic components of the intrinsic barrier ΔG_{int}^*. It is useful to evaluate a preexponential factor, A_{corr}, along with the "real" activation enthalpy, ΔH_r^*. These are obtained from the intercept and slope, respectively, of an Arrhenius plot of $R\ln k_{corr}^\eta$ versus $(1/T)$, where k_{corr}^η represents the temperature-dependent k_{corr} measured at a fixed overpotential η. In view of equation (15b), this preexponential factor can be expressed as

$$A_{corr} = \delta r_e \, \nu_n \, \exp\left(\Delta S_{app}^*/R\right) \tag{16}$$

where the "apparent" activation entropy contains ΔS^*_{int} and any nonunit values of Γ_n and κ_{el}, along with any temperature dependence of these terms. The theoretical values of ΔS^*_{int} have been shown to be small ($\sim 0 \pm 10$ J. deg^{-1} mol^{-1}) on the basis of the conventional dielectric continuum model, although slightly larger values (5 to 15 J. deg^{-1} mol^{-1}) can be obtained from a phenomenological approach which takes into account the experimental entropy changes accompanying electron transfer [17]. The component of ΔS^*_{app} associated with nuclear tunneling, ΔS^*_{nt}, is always negative because Γ_n decreases with increasing temperature [6]. Since this quantity can also be extracted from analytical expressions [1f], relatively reliable calculated values of A_{corr}, A_{calc}, can be obtained from equation (16). In principle, comparison of A_{calc} with the corresponding experimental values enables the importance of nonadiabaticity (i.e., $\kappa_{el} << 1$) and the possible presence of specific solvent work terms to be assessed since neither of these factors are included in A_{calc} (*vide infra*). Alternatively, and equivalently, the comparison between the theoretical and "experimental" activation parameters can be cast in terms of apparent activation entropies, the latter being obtained from experimental data by assuming a particular preexponential factor.

COMPARISONS WITH EXPERIMENTAL DATA

Electrochemical and Homogeneous Rate Parameters in Aqueous Media

The application of the foregoing treatment to transition-metal systems is most straightforward for redox couples containing structurally simple, preferably nonchelating, ligands in order to facilitate calculation of the force constants from vibrational stretching frequencies. Such systems are not overly abundant. Nevertheless, a number of suitable redox couples are provided by octahedral M(III/II) complexes (where M = Ru, Co, Cr, Fe) containing aquo, ammine, ethylenediamine, or polypyridine ligands. Reactions involving these couples have been extensively studied in homogeneous aqueous solution [1d,f]. They might be expected to follow outer-sphere pathways at electrodes as well as in bulk solution since the coordinated ligands are unlikely to bind to metal surfaces.

Table 1 contains cathodic electrochemical rate constants for six aquo, ammine, and ethylenediamine redox couples in aqueous media at mercury, gallium, and lead surfaces, and at upd (underpotential deposited) monolayers of lead and thallium at silver. These surfaces were selected since sufficient equilibrium double-layer data are available within the potential regions where the electrochemical kinetic data were obtained to enable the

TABLE 1

Comparison between observed and calculated rate constants for some outer-sphere electrochemical reactions in aqueous media.

Redox Couple	Metal	$\Delta G^{\circ a}$ kJ mol^{-1}	k_{corr}^{b} cm s^{-1}	A_{corr}^{c} cm s^{-1}	α_{corr}^{d}	k_{calc}^{e} cm s^{-1}	A_{calc}^{f} cm s^{-1}
$Ru(NH_3)_6^{3+/2+}$	Hg	0	2.0	5×10^3	0.6	2.5	2×10^4
$Ru(OH_2)_6^{3+/2+}$	Hg	0	$\sim5\times10^{-2}$			0.3	
$Co(en)_3^{3+/2+\ g}$	Hg	0	2.5×10^{-2}	0.7	~0.8	3×10^{-4}	1×10^4
$Fe(OH_2)_6^{3+/2+}$	Hg	-40	~0.1		0.45	30	
$V(OH_2)_6^{3+/2+}$	Hg	0	8×10^{-4}	1.6×10^3	0.5	4×10^{-3}	2×10^4
		-20	5×10^{-2}	1.6×10^3		0.25	1.7×10^4
	Pb	-20	1.5×10^{-4}		0.4	0.25	
$Cr(OH_2)_6^{3+/2+}$	Hg	0	3×10^{-6}	1.7×10^3	0.50	4×10^{-5}	7×10^3
		-40	1.0×10^{-2}	1.7×10^3	0.50	2×10^{-2}	5×10^3
	Ga	-40	$\sim1.3\times10^{-5}$		~0.5	2×10^{-2}	
	Pb	-40	8×10^{-5}	$\sim5\times10^{-3}$	0.55	2×10^{-2}	5×10^3
	Pb/Ag	-40	7×10^{-3}	$\sim7\times10^{-4}$	0.52	2×10^{-2}	5×10^3
	Tl/Ag	-40	1.3×10^{-3}		0.50	2×10^{-2}	

[a] Free energy of reaction at which listed value of k_{corr} was determined, related to electrode potential E by $\Delta G^{\circ} = F(E-E^{\circ})$, where E° is standard (formal) potential of redox couple (Table 2).

[b] Cathodic work-corrected rate constant at given value of ΔG°; obtained from measured rate constant k_{ob} in $NaClO_4$ and/or KPF_6 electrolytes by using equation (17) (see text). See [11,12,22] for further details.

[c] Work-corrected frequency factor, obtained from intercept of Arrhenius plot of ln k_{corr}^{n} versus (1/T) (see text).

[d] Work-corrected transfer coefficient, determined from $\alpha_{corr} = -(RT/F)(d\ln k_{corr}/dE)$.

[e] Calculated rate constant at given value of ΔG°, obtained from theoretical treatment described in text using thermodynamic and structural data in Table 2.

[f] Calculated frequency factor, obtained from equation (16) as outlined in text.

[g] en = ethylenediamine.

application of reliable electrostatic double-layer corrections [11,12]. This procedure employed the conventional Frumkin relation [18]:

$$\log k_{corr} = \log k_{ob} + (Z - \alpha_{corr})F\phi_r/2.303\ RT \qquad (17)$$

where Z is the reactant charge number, α_{corr} is the work-corrected transfer coefficient, and ϕ_r is the potential at the reaction site. The last quantity was taken as the average potential at the outer Helmholtz plane (o.H.p.), obtained from double-layer compositional data using the Gouy-Chapman model. Although approximate, this approach has been shown to provide self-consistent double-layer corrections for reactants containing ammine and aquo ligands at solid [11,12,19] as well as mercury electrodes [20-23]. Hexafluorophosphate or perchlorate electrolytes were generally employed since these anions exhibit only weak or negligible specific adsorption under the conditions of these experiments. The required double-layer data at mercury and gallium were taken from literature sources; those at the solid surfaces were obtained in this laboratory from differential capacitance measurements [11,12]. Electrolyte conditions were generally selected so to minimize the extent of these corrections, although in some cases the differences between k_{ob} and k_{corr} are substantial (*ca* 10-fold).

The resulting work-corrected electrochemical rate constants, k_{corr}, are listed in Table 1. Experimental details are given elsewhere [11,12,19,22,24]; the techniques were chosen (a.c. polarography, cyclic voltammetry, rotating disk voltammetry, normal pulse polarography) depending upon the magnitude of the rate constants as well as upon the type of surface being studied. For some reactions [$Ru(NH_3)_6^{3+/2+}$, $Ru(OH_2)_6^{3+/2+}$, $Co(en)_3^{3+/2+}$ (en = ethylenediamine)], it is convenient to determine k_{ob} at the formal potential (i.e., where the reductive free energy driving force $\Delta G° = 0$), whereas for the others k_{ob} was determined over a range of cathodic over-potentials (i.e, for negative values of $\Delta G°$). The latter conditions were especially desirable for gallium and the solid metal surfaces in view of their relatively negative dissolution potentials and zero charge potentials. In addition to these rate constants determined at 24°C, experimental values of A_{corr} are given in Table 1. These were obtained from the intercepts of Arrhenius plots of $\ln k_{corr}^\eta$ versus (1/T) as noted above.

Alongside these measured values of k_{corr} and A_{corr} are the corresponding calculated quantities, k_{calc} and A_{calc}. The former were obtained by using the procedure summarized in the preceding section; κ_{el} was taken as unity, and δr_e as 6×10^{-9} cm. {This latter value is the effective reaction zone thickness if $\kappa_{el} \approx 1$ at the plane of closest approach, κ_{el} decreasing exponentially (i.e. the reaction becoming increasing nonadiabatic) for

larger reactant-electrode separation distances [10,25].} The free-energy
barrier ΔG^* and the nuclear frequency factor ν_n were calculated from the
structural and thermodynamic parameters for each redox couple that are given
in Table 2. These structural parameters include the effective reactant
radius, a, the difference in the metal-ligand bond distances between the +3
and +2 oxidation states, Δa, and the corresponding symmetric stretching
frequencies (ν_3, ν_2) and force constants (f_3, f_2) obtained (or estimated)
as described in the footnotes.

These data are also presented in Fig. 2 in the form of a plot of the
experimental electrochemical rate constants, expressed as the work-corrected
unimolecular values, log k_{et}^{corr}, against the corresponding calculated
quantities, log k_{et}^{calc}. Each reaction is shown as a line in Fig. 2 reflect-
ing the range of overpotentials over which k_{corr} data were obtained. Also
shown is the same comparison for fourteen homogeneous outer-sphere reactions
involving pairs of redox couples for which electrochemical kinetic data were
also obtained. Both k_{et}^{corr} and k_{et}^{calc} for the homogeneous reactions were
generated in an entirely analogous manner to those for the electrochemical
reactions (see footnotes to Fig. 1 for details and data sources).

Both Table 1 and Fig. 2 clearly show that the experimental rate constants
for both the electrochemical and homogeneous reactions tend to be signifi-
cantly smaller than the theoretical predictions. However, several systems
show differences between k_{corr} and k_{calc} (or, equivalently, between k_{et}^{corr}
and k_{et}^{calc}) which are less than ten fold or so. These include $Ru(NH_3)_6^{3+/2+}$,
$Ru(OH_2)_6^{3+/2+}$, $V(OH_2)_6^{3+/2+}$, and $Cr(OH_2)_6^{3+/2+}$ at mercury electrodes. Such
relatively minor discrepancies may simply reflect the inevitable uncertain-
ties in the theoretical calculations, especially in the free energy of
activation. Nevertheless, it is interesting to note that the discrepancies
between k_{corr} and k_{calc} for these systems are mirrored by roughly similar
(ca 3 to 10-fold) differences in the corresponding values of A_{corr} and
A_{calc} (Table 1). This suggests that the smaller values of k_{corr} relative
to k_{calc}, at least at mercury, arise primarily from values of κ_{el} somewhat
below unity. Although speculative, this conclusion is supported by a
recent analysis of the relative rates of structurally similar outer- and
inner-sphere Cr(III) reductions at mercury electrodes. This yields an
effective value of $\delta r_e \kappa_{el}$ of ca 0.1 - 0.3 $\overset{o}{A}$ for $Cr(OH_2)_6^{3+/2+}$, suggesting
that $\kappa_{el} \sim 0.2$ at the plane of closest approach [25]. The same analysis
for $Cr(NH_3)_6^{3+}$ reduction indicates that this reaction is adiabatic ($\kappa_{el} \approx 1$)
at the plane of closest approach [25]. This is not surprising given the
demonstrated ability [20] of ammine reactants to approach the metal surface
more closely than the more strongly hydrated aquo complexes [25]. This

TABLE 2

Thermodynamic and structural parameters for transition-metal redox couples.

Redox Couple	$E^{\circ a}$ (mV vs. s.c.e.)	a^b Å	Δa^c Å	ν_3^d cm^{-1}	ν_2^e cm^{-1}	$f_3 \times 10^{-5 f}$ dyne cm^{-1}	$f_2 \times 10^{-5 g}$ dyne cm^{-1}
$Ru(OH_2)_6^{3+/2+}$	15	3.25	0.09±0.01	523[i]	379[j]	2.90	1.52
$V(OH_2)_6^{3+/2+}$	-475	3.25	0.14±0.02	525[k]	379[j]	2.92	1.52
$Fe(OH_2)_6^{3+/2+}$	500	3.25	0.13±0.01	523[k]	379[l]	2.90	1.52
$Cr(OH_2)_6^{3+/2+}$	-660	3.25	0.20±0.03[h]	540[k]	379[j]	3.09	1.52
$Ru(NH_3)_6^{3+/2+}$	-180	3.35	0.04±0.01	500[m]	460[m]	2.65	2.24
$Co(en)_3^{3+/2+}$	-460	4.2	0.21±0.01	485[m]	357[k]	2.44[n]	1.28[n]

[a]Formal potential of redox couple in ionic strength $\mu \sim 0.1$ taken from [38].

[b]Effective average radius of redox couple, taken from [5].

[c]Increase in metal-ligand bond length accompanying reduction of M(III) complex to M(II). Taken from [5], except for $V(OH_2)_6^{3+/2+}$ which was estimated from oxide bond length data using correlation described in [39].

[d]Symmetrical metal-ligand stretching frequency in M(III) complex, measured or estimated as noted.

[e]As in d, but for M(II) complex.

[f]Force constant of metal-ligand bond in M(III) complex, obtained from ν_3 by using equation (9).

[g]As in f, but for M(II) complex.

[h]Average of bond distance changes for axial and equatorial ligands.

[i]Assumed to equal value for $Fe(OH_2)_6^{3+}$ [40].

[j]Assumed to equal value for $Fe(OH_2)_6^{2+}$ [41].

[k]From [40].

[l]From [41].

[m]Determined from surface-enhanced and normal Raman data [37].
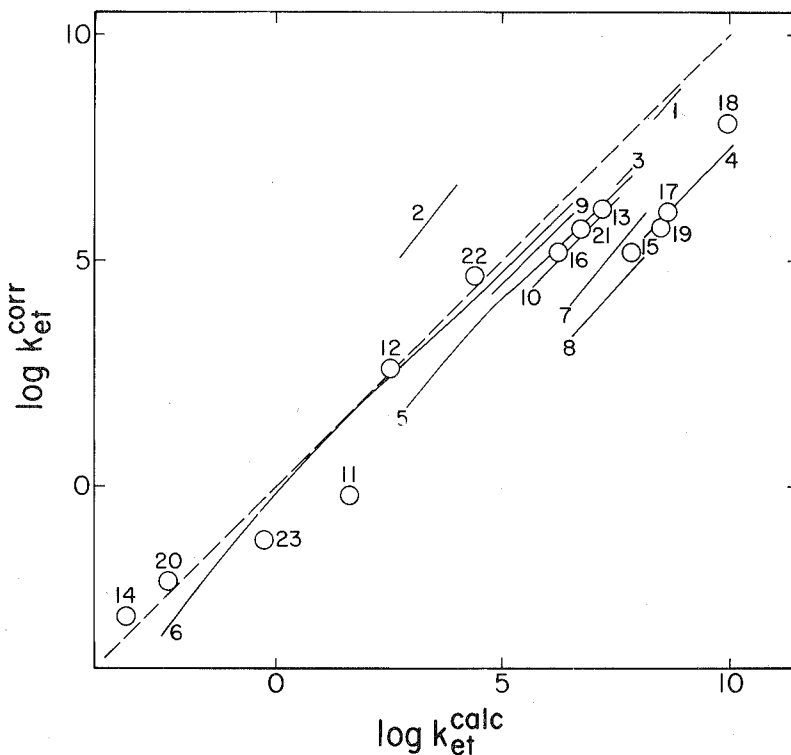
[n]Assumed to equal value for $Co(NH_3)_6^{3+/2+}$ [36].

Fig. 2. Logarithm of experimental work-corrected unimolecular rate constant, log k_{et}^{corr}, for one-electron electrochemical (solid lines) and homogeneous reactions involving transition-metal aquo and ammine complexes in aqueous solution at 25°C, plotted against corresponding quantities, log k_{et}^{calc}, obtained from structural and thermodynamic parameters (Table 2) as outlined in text. Key to systems and data sources (electrochemical reactions shown as reductions, derived from data in Table 1): (1) $Ru(NH_3)_6^{3+/2+}$ - mercury; (2) $Co(en)_3^{3+/2+}$ - mercury; (3) $Ru(OH_2)_6^{3+/2+}$ - mercury; (4) $Fe(OH_2)_6^{3+/2+}$ - mercury; (5) $V(OH_2)_6^{3+/2+}$ - mercury; (6) $Cr(OH_2)_6^{3+/2+}$ - mercury; (7) $Cr(OH_2)_6^{3+/2+}$ - lead; (8) $Cr(OH_2)_6^{3+/2+}$ - gallium; (9) $Cr(OH_2)_6^{3+/2+}$ - upd Pb/Ag; (10) $Cr(OH_2)_6^{3+/2+}$ - upd Tl/Ag; (11) $V(OH_2)_6^{3+} + V(OH_2)_6^{2+}$ [42]; (12) $Fe(OH_2)_6^{3+} + Fe(OH_2)_6^{2+}$ [43]; (13) $Ru(NH_3)_6^{3+} + Ru(NH_3)_6^{2+}$ [44]; (14) $Co(en)_3^{3+} + Co(en)_3^{2+}$ [45]; (15) $Fe(OH_2)_6^{3+} + Ru(OH_2)_6^{2+}$ [46]; (16) $Fe(OH_2)_6^{3+} + Cr(OH_2)_6^{2+}$ [47]; (17) $Fe(OH_2)_6^{3+} + V(OH_2)_6^{2+}$ [48]; (18) $Fe(OH_2)_6^{3+} + Ru(NH_3)_6^{2+}$ [44]; (19) $Ru(OH_2)_6^{3+} + Ru(NH_3)_6^{2+}$ [46]; (20) $Co(en)_3^{3+} + Cr(OH_2)_6^{2+}$ [49]; (21) $Ru(NH_3)_6^{3+} + V(OH_2)_6^{2+}$ [50]; (22) $Ru(NH_3)_6^{3+} + Cr(OH_2)_6^{2+}$ [51]; (23) $Co(en)_3^{3+} + V(OH_2)_6^{2+}$ [49].

result is also consistent with the good agreement seen between k_{corr} and k_{calc} for $Ru(NH_3)_6^{3+/2+}$ at mercury (Table 1).

Nevertheless, the substitution of upd lead and thallium, and especially lead and liquid gallium, surfaces for liquid mercury yields substantial (up to ca 10^3-fold) decreases in k_{corr} even though no changes are predicted by theory (Table 1). These rate decreases are accompanied by comparable or larger decreases in A_{corr}. (Although the data presented in Table 1 are somewhat sparse in this regard, much the same behavior has been observed for a number of other aquo and ammine reactants under these conditions [11,12].) A likely explanation for this surprising behavior lies in the anticipated differences in solvent structure at these metal surfaces. Mercury is known to provide a "hydrophobic" surface in that it exhibits only a small tendency to adsorb water molecules via the oxygen atom [26]. In contrast, lead and especially gallium are relatively "hydrophilic" in that they strongly adsorb water molecules [26]. These differences are accentuated at a given electrode potential, especially in the region where the data in Table 1 were obtained (ca -800 to -1100 mV. vs s.c.e.), since upd lead, thallium, lead, and gallium surfaces all have small positive or negative electronic charges, whereas mercury carries a large negative charge. Consequently, the latter surface should present a relatively mild solvent "structure making" environment [26] in which the secondary hydration surrounding the cationic reactants will remain undisturbed. This hydration shell may be severely perturbed in the vicinity of the other four surfaces due to their marked tendency to orient water molecules in the opposite direction to that desired by the incoming reactant [26].

Mercury may therefore provide an unusually "mild perturbing" environment for such outer-sphere reactions, therefore accounting for the good agreement between the calculated and experimental rate parameters at this surface (Table 1). The significantly different rate parameters seen at the other four, "strongly perturbing", surfaces may therefore be due to unfavorable work terms associated with the differing solvent structure in the bulk and interfacial environments, possibly accompanied by more nonadiabatic pathways (i.e., smaller κ_{el}).

Evidence favoring the former factor is obtained by examining the corresponding experimental and calculated rate parameters for related homogeneous reactions. Comparisons between the experimental and calculated rate constants (Fig. 2) show similar discrepancies to those seen for the electrochemical reactions. Furthermore, the experimental frequency factors A_{corr} are typically 10^3 - 10^4 fold smaller than the theoretical predictions [27]. (This result has more commonly been expressed in terms of apparent observed

activation entropies which are ca 60-80 J. deg^{-1} mol^{-1} more negative than those predicted from theory [28].) These discrepancies may well be associated with the changes in solvation that occur as the reactant approaches the "hydrophilic" cationic coreactant [28]. The factors giving rise to the observed discrepancies between the experimental and calculated rate parameters at hydrophilic surfaces and at cationic reaction sites in bulk solution may therefore have a common origin.

Table 1 also contains work-corrected cathodic transfer coefficients, α_{corr}, obtained from $\alpha_{corr} = -(RT/F)(d\ln k_{corr}/dE)$. The values of α_{corr} for the aquo reactants are uniformly around 0.50 for $\Delta G° \leq 0$, close to the corresponding theoretical values, α_{calc} (0.45 - 0.55). Although α_{corr} values for $Cr(OH_2)_6^{3+/2+}$ and $V(OH_2)_6^{3+/2+}$ do not exhibit the significant dependence upon the cathodic overpotential that is anticipated from equation (13), substantial decreases in the anodic transfer coefficient for these reactions occur with increasing anodic overpotential [22]. This behavioral difference at cathodic and anodic overpotentials is qualitatively explicable in terms of the anticipated asymmetry in the potential-energy surfaces resulting from the difference in force constants between the oxidized and reduced states (Table 2; Fig. 1). The larger values of α_{corr} for $Ru(NH_3)_6^{3+/2+}$ and especially $Co(en)_3^{3+/2+}$ suggest that the reaction site for these complexes lies inside the o.H.p., as might be anticipated from their weaker hydration (*vide supra*) [20,21]. However, the observation that $k_{corr} \gg k_{calc}$ and $A_{corr} \ll A_{calc}$ for $Co(en)_3^{3+/2+}$ (Table 1) suggests that this reaction does not occur by a simple outer-sphere mechanism at mercury electrodes. It seems likely that the relatively hydrophobic ethylenediamine ligands are able to replace inner-layer water molecules (i.e., are adsorbed) at the mercury-aqueous interface. Evidence for such adsorption is contained in a.c. polarograms for this system [29].

Solvent Dependence of Electrochemical Rate Parameters

The conventional treatment of the outer-shell solvent employed above is based on a dielectric continuum model [equation (7)]. This model may well be seriously oversimplified, especially for reactants that interact strongly with the solvent. Variation of the bulk solvent composition may also influence the rate parameters via alterations in the interfacial solvent structure. Such solvent effects are best examined for transition-metal systems by selecting substitutionally inert redox couples so that the inner-shell composition, and hence $\Delta G^*_{is,int}$, remains constant as the solvent is varied. We have studied the solvent dependence of k_{corr}^S for

TABLE 3

Solvent dependence of standard electrochemical rate constants for $Ru(NH_3)_6^{3+/2+}$ and $Co(en)_3^{3+/2+}$ at mercury electrodes.

Redox Couple	Solvent[a]	k_{ob}^s [b] cm s^{-1}	A_{corr} [c] cm s^{-1}	k_{corr}^s [d] cm s^{-1}	k_{calc}^s [e] cm s^{-1}	DN[f]
$Ru(NH_3)_6^{3+/2+}$	H_2O	0.35[g]	5×10^3	2.0	2.5	~18
	PC	0.6[h]		~3	5	15.1
	DMF	0.35[h]	25	0.25	10	26.6
	DMSO	6.5×10^{-2} [h]	2.5×10^2	5×10^{-2}	15	29.8
$Co(en)_3^{3+/2+}$	H_2O	3×10^{-2} [i]	0.7	2.5×10^{-2}	3×10^{-4}	~18
	F	3×10^{-3} [i]	8×10^5	1.5×10^{-3}	7×10^{-4}	~24
	NMF	5×10^{-3} [i]	2×10^6	6×10^{-4}	7×10^{-4}	27
	PC	4.5×10^{-3} [i]		3×10^{-4}	7×10^{-4}	15.1
	AN	1×10^{-3} [i]	2×10^5	1.5×10^{-3}	5×10^{-4}	14.1
	DMF	3×10^{-3} [i]	2.5×10^6	1×10^{-5}	1.2×10^{-3}	26.6
	DMSO	1.5×10^{-3} [i]	1×10^7	~1×10^{-5}	2×10^{-3}	29.8

[a] PC = propylene carbonate, DMF = N,N-dimethylformamide, DMSO = dimethyl-sulfoxide; F = formamide, NMF = N-methylformamide, AN = acetonitrile.

[b] Observed standard rate constant (i.e. at formal potential), measured in specific electrolyte. For details see [24, 30, and 33].

[c] Work-corrected frequency factor, obtained from intercept of Arrhenius plot of $\ln k_{corr}^s$ versus $(1/T)$ (see text).

[d] Work-corrected standard rate constant, obtained from k_{ob}^s by using equation (17) (see text). For details see [24, 30, and 33].

[e] Calculated standard rate constant, obtained from theoretical treatment described in text using thermodynamic and structural data in Table 2. Values of R_e [equation (7)] taken as 14 Å in water and ca 17 Å in other solvents [30].

[f] Solvent "donor number", from V. Gutmann, "The Donor-Acceptor Approach to Molecular Interactions", Plenum, N.Y., 1978, Chapter 2.

[g] Determined in 0.1 M KPF_6.

[h] 0.05 M tetrabutylammonium hexafluorophosphate.

[i] 0.1 M tetraethylammonium perchlorate or 0.1 M KPF_6.

$Co(en)_3^{3+/2+}$ at mercury electrodes [30,31]. Some of these data are summarized in Table 3, along with corresponding, previously unreported, values of A_{corr} and the theoretically predicted rate constants, k_{calc}^S.

The substantial (ca 10^3-fold) decreases in k_{corr}^S seen upon substituting aprotic solvents for water contrasts sharply with the small increases in k_{calc} predicted from the dielectric continuum treatment (Table 3). The former have been ascribed to increases in the outer-shell reorganization energy associated with short-range reorientation of solvent molecules, together with decreases in κ_{el} [30]. However, neither explanation is entirely consistent with the additional information given in Table 3. Thus, the values of k_{corr}^S obtained for $Co(en)_3^{3+/2+}$ are in closer agreement with the corresponding values of k_{calc}^S in nonaqueous solvents than in water. Moreover, these smaller values of k_{corr}^S in nonaqueous media are accompanied by markedly larger A_{corr} values [31] (Table 3). Taken together, these data suggest that the solvent dependence of k_{corr}^S is connected with the varying ability of these different media to solvate the reacting species within the double layer and prevent it from being adsorbed (i.e., replacing the inner-layer solvent).

This conclusion, albeit speculative, is supported by a roughly inverse correlation between ln k_{corr}^S and the solvent donor number (DN), also listed in Table 3. We have shown that there is a similar correlation between the redox thermodynamics for ammine and ethylenediamine couples and DN, arising from donor-acceptor interactions between surrounding solvent molecules and the acidic ammine hydrogens [32]. This remarkably large solvent effect may also be due in part to the influence of specific reactant-solvent interactions upon the intrinsic outer-shell reorganization energy. This latter factor may be responsible for the markedly (20-30 fold) smaller values of k_{corr}^S compared to k_{calc}^S in dimethylformamide (DMF) and dimethylsulfoxide (DMSO) (Table 3). Some support for this assertion is obtained from the dependence of k_{corr}^S for $Ru(NH_3)_6^{3+/2+}$ at mercury electrodes upon the solvent; some data recently obtained for this system [33] are given in Table 3. As for $Co(en)_3^{3+/2+}$, the k_{corr}^S for $Ru(NH_3)_6^{3+/2+}$ is strongly solvent dependent, with $k_{corr}^S \ll k_{calc}^S$ in DMF and especially DMSO.

These data therefore suggest that the dielectric continuum model may significantly underestimate the solvent reorganization energy for redox couples such as $Ru(NH_3)_6^{3+/2+}$ and $Co(en)_3^{3+/2+}$ in DMSO and DMF where extensive changes in short-range structure are known to accompany electron transfer [30]. This matter will be considered in detail elsewhere [33].

332

CONCLUDING REMARKS

Although not particularly extensive, the foregoing comparisons illustrate some major virtues of undertaking absolute as well as relative tests of electron-transfer theory for electrochemical reactions. Despite the provocative assertions of some [34], contemporary theory can yield reasonable agreement with experimental data at least for some outer-sphere reactions at mercury electrodes. Nevertheless, a number of interesting discrepancies remain. The common finding that $k_{corr} < k_{calc}$ and $A_{corr} < A_{calc}$ probably arises in part from nonadiabaticity, i.e., $\kappa_{el} < 1$. The relative importance of other factors is difficult to gauge at present. The solvent reorganization barrier may often be significantly larger than that predicted from the dielectric continuum model. The observed discrepancies between experiment and theory may be associated as much with the limitations of electrostatic models in estimating the work terms (i.e., "double-layer" effects) as with the deficiencies of the electron-transfer model itself. However, parallel discrepancies between experiment and theory are also seen with ferricinium-ferrocene redox couples at electrodes in solution for which the work terms are liable to be small [35].

It would clearly be desirable to refine the theoretical models further as they pertain to electrochemical as well as homogeneous outer-sphere reactions, especially with regard to the electron-tunneling aspects. Nevertheless, the kinetic formalisms underlying the present theoretical treatment offer considerable, so far unexploited, opportunities for examining the fundamental features of electrochemical and homogeneous processes on a common basis. In turn, such activities should spur the acquisition of the further electrochemical kinetic data, including activation parameters as well as rate constants, that is critical to the development of a truly molecular-based understanding of electrode processes.

REFERENCES

1   For recent reviews, see (a) P. P. Schmidt, Spec. Period Rep., Electro-
    chemistry, The Chemical Society, Vol. 5, Chapter 2 (1975); Vol. 6,
    Chapter 4 (1977); (b) J. Ulstrup,"Charge Transfer Processes in Condensed
    Media", Springer-Verlag, Berlin, 1979; (c) R. R. Dogonadze, A. M.
    Kuznetsov, T. A. Marsagishvili, Electrochim. Acta, 25 (1980) 1;
    (d) R. D. Cannon, "Electron-Transfer Reactions", Butterworths, London,
    1980; (e) M. D. Newton, Int. J. Quant. Chem. Symp.,14 (1980) 363;
    (f) N. Sutin, Prog. Inorg. Chem.,30 (1983) 441.
2   M. J. Weaver, in J. J. Zuckerman,(Ed.),"Inorg. Reactions and Methods",
    Chemie Verlag, in press.
3   R. A. Marcus, J. Chem. Phys.,43 (1965) 679; R. A. Marcus, in P. A.
    Rock,(Ed.),"Spec. Topics in Electrochemistry", Elsevier, New York,
    1977, Chapter 4.
4   L. E. Bennett, Prog. Inorg. Chem.,18 (1973) 1.
5   B. S. Brunschwig, C. Creutz, D. H. MaCartney, T.-K Sham and N. Sutin,
    Disc. Far. Soc.,74 (1982) 113.
6   B. S. Brunschwig, J. Logan, M. D. Newton and N. Sutin, J. Am. Chem.
    Soc., 102 (1980) 5798.
7   (a) G. M. Brown and N. Sutin, J. Am. Chem. Soc.,101 (1979) 883; (b)
    N. Sutin and B. S. Brunschwig, ACS Symp. Ser.,198 (1982) 105.
8   R. A. Marcus, Int. J. Chem. Kinetics,13 (1981) 865.
9   T. T.-T. Li, M. J. Weaver and C. H. Brubaker, J. Am. Chem. Soc.,104
    (1982) 2381.
10 J. T. Hupp and M. J. Weaver, J. Electroanal. Chem.,152 (1983) 1.
11 H. Y. Liu, Ph.D. dissertation, Michigan State University, 1982.
12 J. T. Hupp, Ph.D. dissertation, Michigan State University, 1983.
13 M. D. Newton, ACS Symp. Ser.,198 (1982) 255.
14 B. L. Tembe, H. L. Friedman and M. D. Newton, J. Chem. Phys.,76
    (1982) 1490.
15 M. J. Weaver, J. Phys. Chem.,80 (1976) 2645; ibid., 83 (1979) 1748;
    Israel J. Chem.,18 (1979) 35.
16 J. T. Hupp and M. J. Weaver, J. Electroanal. Chem.,145 (1983) 43;
    T. T.-T. Li, K. L. Guyer, S. W. Barr and M. J. Weaver, J. Electroanal.
    Chem., 164 (1984) 27.
17 J. T. Hupp and M. J. Weaver, J. Phys. Chem., in press.
18 M. J. Weaver, J. Electroanal. Chem.,93 (1978) 231.
19 K. L. Guyer, S. W. Barr, R. J. Cave and M. J. Weaver, in S.
    Bruckenstein, J. D. E. McIntyre, B. Miller, E. Yeager (Eds.),"Proc.
    3rd Symp. on Electrode Processes", Electrochemical Society, 1980,
    p. 390.
20 M. J. Weaver and T. L. Satterberg, J. Phys. Chem.,81 (1977) 1772.
21 T. L. Satterberg and M. J. Weaver, J. Phys. Chem.,82 (1778) 1784.
22 P. D. Tyma and M. J. Weaver, J. Electroanal. Chem.,111 (1980) 195.
23 M. J. Weaver, H. Y. Liu and Y. Kim, Can. J. Chem.,59 (1981) 1944.
24 T. Gennett and M. J. Weaver, Anal. Chem., submitted.
25 J. T. Hupp and M. J. Weaver, J. Phys. Chem., in press.
26 (a) S. Trassati, in B. E. Conway, J. O'M. Bockris (Eds.),"Modern
    Aspects of Electrochemistry", Vol. 13, Plenum Press, N.Y., 1979,
    p. 81; (b) S. Trassati, Electrochim. Acta,28 (1983) 1083.
27 J. T. Hupp and M. J. Weaver, in preparation.
28 M. J. Weaver and E. L. Yee, Inorg. Chem.,19 (1980) 1936.
29 (a) P. A. Lay and J. T. Hupp, unpublished observations; H. A. Laitinen
    and J. E. B. Randles, Trans. Far. Soc.,51 (1955) 54.
30 S. Sahami and M. J. Weaver, J. Electroanal. Chem.,124 (1981) 35.
31 J. K. Farmer and M. J. Weaver, unpublished results.
32 S. Sahami and M. J. Weaver, J. Electroanal. Chem.,122 (1981) 171.
33 T. Gennett, J. T. Hupp and M. J. Weaver, in preparation.
34 J. O'M. Bockris and S. U. M. Khan, "Quantum Electrochemistry", Plenum,
    New York, 1979.

35   T. Gennett and M. J. Weaver, in preparation.
36   K. H. Schmidt and A. Muller, Inorg. Chem.,14 (1975) 21ʃ
      Chem. Revs.,19 (1976) 41.
37   M. A. Tadayyoni, S. Farquharson and M. J. Weaver, J. Ch
      press.
38   E. L. Yee, R. J. Cave, K. L. Guyer, P. D. Tyma and M. J. .
      Chem. Soc.,101 (1979) 1131.
39   J. K. Beattie, S. P. Best, B. W. Skelton and A. H. White, J. Chem. Soc
      Dalton,(1981) 2105.
40   S. P. Best, J. K. Beattie and R. S. Armstrong, J. Chem. Soc. Dalton,
      submitted.
41   T. E. Jenkins and J. Lewis, Spectrochim. Acta, A37 (1981) 47.
42   K. V. Krishnamurty and A. C. Wahl, J. Am. Chem. Soc., 80 (1958) 5921.
43   J. Silverman and R. W. Dodson, J. Phys. Chem.,56 (1952) 846.
44   T. J. Meyer and H. Taube, Inorg. Chem.,7 (1968) 2369.
45   F. P. Dwyer and A. M. Sargeson, J. Phys. Chem.,65 (1961) 1892.
46   W. Bottcher, G. M. Brown and N. Sutin, Inorg. Chem.,18 (1979) 1447.
47   G. Dultz and N. Sutin, J. Am. Chem. Soc.,86 (1964) 829.
48   A. Ekstrom, A. B. McLaren and L. E. Smythe, Inorg. Chem. 15 (1976)
      2853.
49   T. J. Przystas and N. Sutin, J. Am. Chem. Soc.,95 (1973) 5545.
50   C. A. Jacks and L. E. Bennett, Inorg. Chem.,13 (1974) 2035.
51   J. F. Endicott and H. Taube, J. Am. Chem. Soc.,86 (1964) 1686.